Localization and Visualization of Pulmonary Emboli with Radiolabeled Fibrin-Specific Monoclonal Antibody

Michito Kanke, Gary R. Matsueda, H. William Strauss, Tsunehiro Yasuda, Chiau-Suong Liau, and Ban An Khaw

Division of Nuclear Medicine and the Cardiac Unit, Massachusetts General Hospital, Boston, Massachusetts

Indium-111-labeled monoclonal antibody 64C5 specific for the beta-chain of fibrin monomer was used to image canine (n = 6) experimental pulmonary emboli (at least one barium-thrombin and one copper-coil induced clot per dog). Uptake of ^{111}In-64C5 and ^{125}I-control-DIG26-11 were compared in 10 clots (7 barium-thrombin and 3 copper-coil) identified in the lungs. There was no difference in the blood clearance of ^{111}In-64C5 and ^{125}I-DIG26-11. Uptake of ^{111}In-64C5 (0.183 ± 0.105, mean %ID/g) was greater than ^{125}I-DIG26-11 (0.024 ± 0.025) in pulmonary clots ($p < 0.001$). Mean thrombus to blood ratios at 24 hr were 6.78:1 for 64C5 and 0.57:1 for DIG26-11. The clots visualized in vivo were larger (0.315 ± 0.381 g) than clots not visualized (0.089 ± 0.098). Negative images were recorded in three dogs with pulmonary emboli, injected with ^{111}In-labeled control monoclonal antibody 3H3. These data suggest that ^{111}In-labeled antifibrin can detect large pulmonary emboli in vivo.

J Nucl Med 1991; 32:1254–1260

Detection of pulmonary embolism is a clinically vexing problem due to the nonspecific history and physical findings usually associated with the condition. Laboratory procedures frequently are required to make the diagnosis. The radionuclide ventilation/perfusion lung scan is helpful for the detection of large, occlusive emboli in patients with relatively normal lungs. In patients with obstructive lung disease, abnormalities of perfusion may be due to regional hypoxia, superimposed pulmonary emboli, or both, making it difficult to identify the etiology of reduced perfusion. Alderson et al. reported that in dogs with experimental pulmonary emboli only 5 of 19 angiographically nonocclusive emboli produced lesions on lung scans (*1*).

The problems inherent in ventilation/perfusion imaging for detection of pulmonary embolism may be overcome if a radiolabeled clot seeking-specific agent could be used instead of a flow indicator. These agents would have the theoretical advantages of directly identifying the thrombus, not its secondary effect on pulmonary perfusion, and would not be influenced by other causes of decreased regional perfusion, such as local hypoxia. Previously, investigators have suggested radiolabeled platelets (*2*) or fibrinogen (*3*) for imaging emboli. Both radiopharmaceuticals worked well in animals with acute thrombus. Unfortunately, when tested in human subjects, neither radiopharmaceutical localized in emboli quickly, or with sufficient avidity to permit reliable detection of pulmonary emboli. In 1965 and 1969, Spar and his colleagues described the use of a polyclonal antibody to fibrinogen that also cross-reacted with fibrin for detection of deep venous thrombi and left atrial thrombus in a patient (*4,5*). While the concept was attractive, additional clinical studies were not successful, possibly due to cross-reactivity of this antibody with circulating fibrinogen, which removed a large fraction of the antibody before it could interact with the preformed thrombus. The recent description of a family of highly specific monoclonal antibodies directed against the beta-chain of fibrin (*6,7*), with virtually no cross-reactivity to fibrinogen, presents a unique opportunity to determine if "hot spot" imaging of pulmonary emboli is feasible. Initial studies using radiolabeled anti-fibrin by different investigators demonstrated the ability of these antibodies to detect venous thrombi in both animals and man (*8–12*). This study reports our experience with a specific anti-fibrin antibody for the detection of experimental pulmonary emboli in dogs.

METHODS

Production of Fibrin-Specific Monoclonal Antibodies

A peptide (15–21 amino acids) homologous to the n terminal amino acid sequence of the beta-chain of the fibrin monomer was synthesized (*13,14*) and used as an immunogen for immunization to produce monoclonal antibodies specific for fibrin. Briefly, BALB/c mice were immunized with the synthetic peptide covalently linked to a carrier keyhole-lympet hemocyanin (*6*). The hybridoma cells were generated by polyethylene glycol fusion of murine myeloma SP2/0A cells with the immune spleen cells. The hybridomas were selected on the basis of fibrin monomer specificity. Monoclonality was achieved by multiple subcloning

Received Aug. 7, 1990; revision accepted Dec. 5, 1990.

For reprints contact: Ban An Khaw, PhD, Division of Nuclear Medicine, Tilton-2, Massachusetts General Hospital, Fruit St., Boston, MA 02114.

utilizing the limiting dilution procedure. The antibody designated 64C5 produced by one of the monoclonal cell lines was observed to be highly specific for the beta-chain of fibrin. It did not cross-react with the alpha-chain of the fibrin monomer nor with native fibrinogen (*6*). The monoclonal antibody 64C5 was subsequently produced in large concentrations in the ascites form and purified by protein-A immunoadsorbtion (*15*). Purity was confirmed by 7% SDS polyacrylamide gel electrophoresis (*16*), which showed presence of only light and heavy chains of the immunoglobulin. 64C5 was determined by subclass specific reagents to be of IgG_1,k isotype.

A murine monoclonal antibody (DIG26-11, $IgG_{2a}k$, directed against digoxin or 3H3 (IgG_1,k) specific for cardiac myosin but not specific or fibrin or fibrinogen, was used as controls.

Radiolabeling Methods

1. The antibody was labeled with ^{111}In- via diethylene triamine pentaacetic acid (DTPA), which has been covalently attached to 64C5 by the mixed anhydride method as previously described (*17*). Indium-111 labeling was achieved by addition of 37–74 MBq ^{111}In-chloride in 0.1–0.5 *M* citrate pH 5.5 to 1–4 mg of DTPA-64C5. After 15–30 min incubation at room temperature, the reaction mixture was chromatographed on a sephadex G-25 10-ml column equilibrated with lactated ringers solution. Indium-111-labeled 64C5 was eluted in the void volume.

2. Radioiodination by ^{125}I was performed with the lactoperoxidase procedure of Marchalonis (*18*). Free and labeled ^{125}I were separated by sephadex G-25 column chromatography (10 ml column).

Indium-111-labeled 64C5 was used within 2 hr of labeling in experimental canine studies. An aliquot of ^{111}In-64C5 was submitted for in vitro analysis of antifibrin antibody activity relative to ^{125}I-labeled 64C5.

Experimental Protocol

The experimental protocol is represented diagrammatically in Figure 1. Six mongrel dogs weighing 20–24 kg were anesthetized by intravenous sodium pentobarbitol (30 mg/kg), intubated, and respiration was maintained on a Harvard respirator. Sterile surgical techniques were used throughout the remainder of the experimental protocol. A segment of the left jugular vein, approximately 3 cm in length, was dissected and proximal and distal ties made using 2-0 silk sutures. An incision 3–5 mm length was made in the distal portion of the isolated venous segment. Then a thrombogenic copper-coil, approximately 3–5 mm long, 2–3 mm diameter, weighing about 30 mg, was inserted into the vein. This incision was closed using 4-0 sutures, and the restraining ligatures were removed to allow passage of the coil into the lungs. Thirty minutes after release of the copper-coil, a 2–3-cm length of the jugular segment was re-isolated and ligated proximal to the initial incision site. Using a tuberculin syringe fitted with a 27-gauge needle, approximately 100 mg of barium sulfate were mixed with 1 ml of canine blood and injected into the isolated venous segment followed by 50–100 units of human thrombin. The clot thus formed was allowed to age for 30 min, the ties were released, and the clot was dislodged into the proximal jugular vein. Each animal was then placed on an intravenous infusion of 1,250 mg aminocaproic acid (AMICAR) in 250 ml saline to reduce thrombolysis. Approximately 30–45 minutes after the clot release, a mixture of ^{111}In-labeled antifibrin antibody (18.5 MBq in ~500 μg DTPA-64C5) and ^{125}I-labeled nonfibrin-specific monoclonal antibody control (~3–4 MBq in ~100 μg) was administered intravenously. At this time, 5,000 units of heparin were injected intravenously. An aliquot of the antibody mixture was saved as a standard for in-vitro counting.

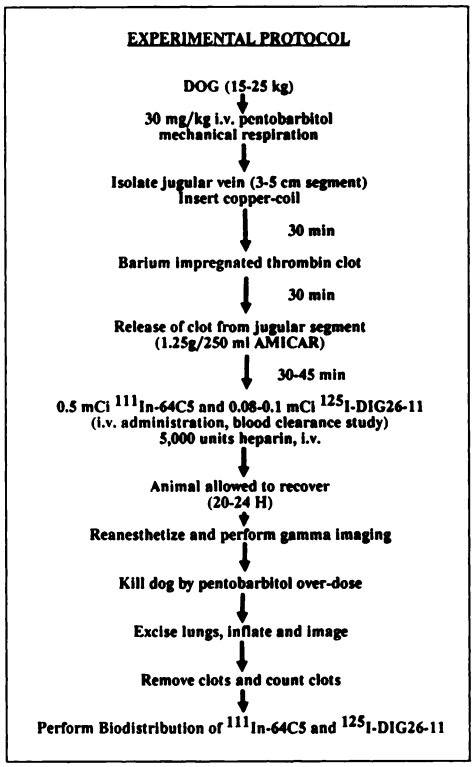

FIGURE 1. Flow chart of the experimental protocol used to study localization and visualization of ^{111}In-64C5 and ^{125}I-DIG26-11 in canine experimental pulmonary emboli.

After administration of the antibodies, the animals were allowed to recover from anesthesia overnight in a recovery cage. In addition, three more dogs were used to study blood clearance of the ^{111}In-64C5. In these dogs, the copper-coil and the barium clots were made in the femoral veins. The rest of the protocol was identical to that previously described.

Another three dogs with experimental pulmonary emboli induced with thrombin impregnated clots, injected with ~20 MBq of ^{111}In-non-antifibrin specific monoclonal antibody 3H3 (~0.5 mg), were used as controls for comparison of the images. In this study, only the anterior view was taken.

In Vivo Imaging

Approximately 20–24 hr after the administration of the antibodies, the animals were reanesthetized and the thoracic region was imaged using a portable gamma camera (Ohio Nuclear 420) with a medium-energy collimator. Multiple view images were recorded with the pulse-height analyzer set for both peak energies of ^{111}In at 173 keV and 246 keV, with a 50% window.

Blood Clearance

Serial blood samples (~1 ml aliquots) were obtained at multiple time points ranging from 1 min to 24 hr after injection to determine blood clearance. The samples were first weighted and then were counted at the conclusion of each experiment in a gamma scintillation counter (LKB Wallace 1282 Compugamma universal gamma counter, Wallace Oy, Finland). The initial blood sample obtained at 1 min was used as the 100% reference activity of the administered dose.

Pathology of Pulmonary Clots

At the conclusion of in-vivo imaging, the dogs were killed by an overdose of pentobarbitol. The lungs were carefully excised and inflated with air to approximate their in-vivo size. The inflated lungs were imaged. Radiographs were also obtained for each set of lungs to visualize the location of the barium clots and the copper-coils. After determination of clot location, the pulmonary arteries were dissected and the clots were removed, weighed, and counted.

Tissue Biodistribution

Immediately after the dogs were killed by pentobarbitol overdose, approximately 1 g duplicate samples of the heart muscle, lungs, liver, kidney, and skeletal muscles were obtained for determination of radiotracer biodistribution. The tissue samples were weighed and then counted in a gamma counter (Compugamma, LKB) utilizing a setting of 150–300 keV for ^{111}In (to include both energy peaks) and a setting of 20–50 keV for ^{125}I. Duplicate 10-μl aliquots of ^{111}In-64C5 and ^{125}I-Dig26-11 were included with each set of tissue samples to be counted and were used as standards for calculation of the injected doses and for automatic correction of cross-talk. The raw data were calculated as cpm/g tissue as well as percent of injected dose per gram (%ID/g). Tissue uptake represented as %ID/g was calculated by the following equation:

$$\%ID/g = [(A/W)/I] \times 100,$$

where A = tissue count (cpm), W = tissue weight (g), and I = total injection dose (cpm).

Statistical Analyses

Linear regression analyses were fit utilizing Statgraphic version 2.6 (Statistical Graphics Corp.).

RESULTS

Blood Clearance

Figure 2 shows the 24-hr blood clearance of ^{111}In-64C5 and ^{125}I-DIG26-11. There was no significant difference between the blood clearance of ^{111}In-64C5 and the control ^{125}I-DIG26-11. Blood clearance was fit to the curve described by the equation: $Y = 22.46e^{(-0.2369*X)} + 80.31e^{(-0.0008171*X)}$ ($p < 0.001$, $r = 0.99$). The half-life of the fast component was 2.9 min and the half-life of the slow component was 14.1 hr.

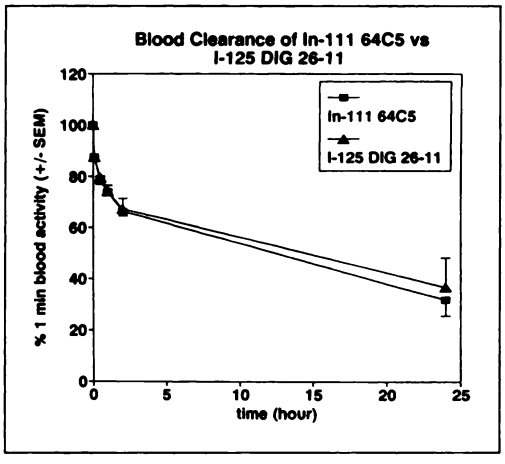

FIGURE 2. Comparison of blood clearance of ^{111}In-64C5 (boxes) to control ^{125}I-DGI26-11 (triangles) in dogs (n = 6) for 24 hr postintravenous administration of the radiolabeled antibodies. The vertical bars represent ± s.e.m. $Y = 22.46e^{(-0.2369*X)} + 80.31e^{(-0.0008171*X)}$ ($p < 0.001$, $r = 0.99$). The half-life of the fast component was 2.9 min and the half-life of the slow component was 14.1 hr.

Biodistribution

Figure 3 shows tissue distribution of ^{111}In-64C5 and ^{125}I-DIG26-11. The uptakes of ^{111}In-64C5 and ^{125}I-DIG26-11 in the pulmonary clots represented as mean %ID/g were 0.183 ± 0.105 (mean ± s.e.) and 0.024 ± 0.025, respectively. Uptake of ^{111}In-64C5 in pulmonary clots was significantly greater than that of ^{125}I-DIG26-11 ($p < 0.001$). The data suggest that ^{111}In-64C5 binds specifically in vivo to pulmonary clots. The ratio of the means of %ID/g of ^{111}In-64C5 to ^{125}I-DIG26-11 in the pulmonary clots was 7.63:1. The ratio of the means of the specific antibody activity in the thrombi (%ID/g) to blood activity (%ID/g) at 24 hr was 6.78:1, whereas the corresponding ratio of the means of nonspecific antibody activity in the same thrombi-to-blood activity (%ID/g) also at 24 hr was 0.571:1.

Identification of Pulmonary Clots

Ten clots were identified in the pulmonary arteries by ex vivo imaging and from the radiographs of the excised and inflated lungs. The range of clot weights was 4 to 974 mg (mean = 202 mg). The mean uptake of radiotracers in these clots was 0.183 ± 0.105 %ID/g (mean ± s.e.m.). Seven of the ten clots were barium clots and the other three were copper-coil clots. There was no significant difference between ^{111}In uptake in the barium clots and the copper-coil clots. Figure 4A shows the correlation between % injected dose of ^{111}In-64C5 per gram of clot to weight of the clots. There is an inverse exponential relationship between %ID/g of ^{111}In-64C5 and the clot size in

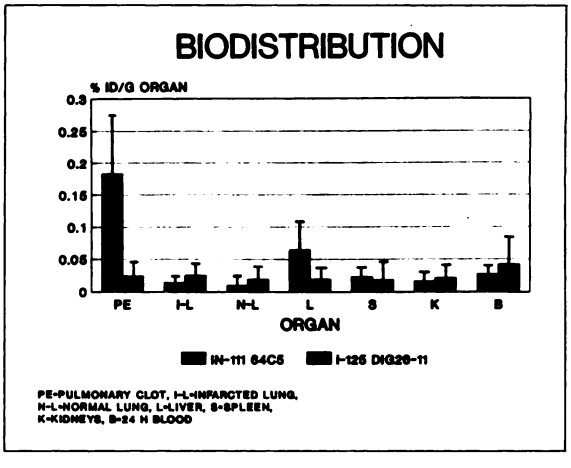

FIGURE 3. Biodistribution of ^{111}In-64C5 and ^{125}I-DIG26-11 represented as %ID/g of each organ in the pulmonary clots (PE), infarcted lung (I-L), normal lung (N-L), liver (L), spleen (S), kidneys (K), and the 24-hr blood sample (B). The vertical bars represent ± s.e.m.

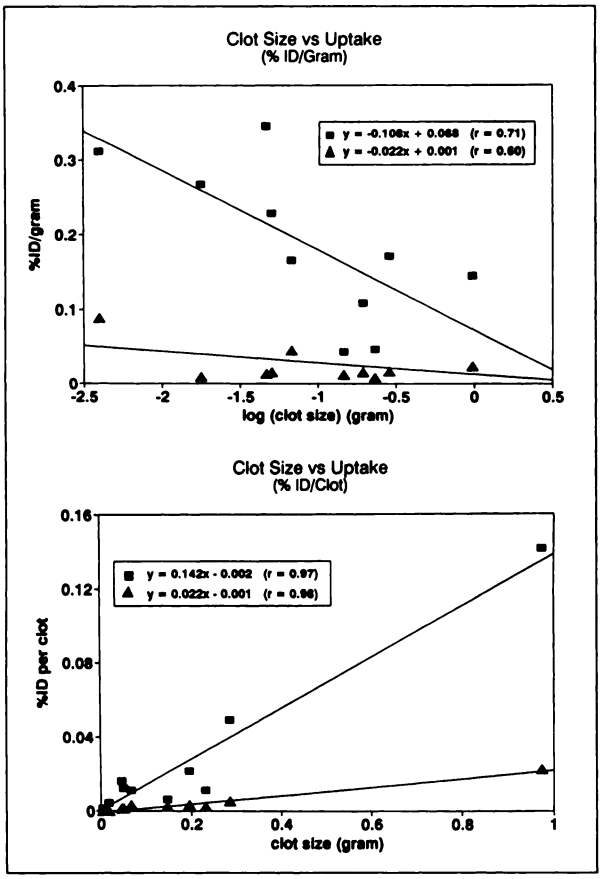

FIGURE 4. (A) Correlation between log of clot size in grams (x-axis) to uptake of ^{111}In-64C5 and or ^{125}I-DIG26-11 in % injected dose per gram (y-axis, %ID/g). An inverse exponential relationship between clot size and ^{111}In-64C5 uptake was obtained (boxes, %ID/g = 0.067 − 0.108 log[clot size], r = 0.71). The relationship between clot size and ^{125}I-DIG26-11 uptake was %ID/g = 0.001 − 0.022 log[clot size], r = 0.60 (triangles). (B) Correlation between clot size in grams (x-axis) to %ID (y-axis) in each clot for uptake of ^{111}In-64C5 and ^{125}I-DIG26-11. A linear relationship was obtained between clot size and %ID of ^{111}In-64C5/clot (boxes, y = −0.0016 + 0.142x, r = 0.97). The relationship between %ID/clot to clot size for ^{125}I-DIG26-11 was y = 0.022x − 0.001, r = 0.98 (triangles). However, the best fit line of identity was almost parallel to the x-axis.

grams (y = a + bx, where y = %ID/g ^{111}In-64C5, x = log (clot size in grams), a = 0.068 ± 0.048 (±s.e.) and b = −0.108 ± 0.049, r = 0.71). On the other hand, a linear relationship was obtained between %ID/clot (y) and the clot size (x), (y = 0.142x −0.002, r = 0.97, p < 0.00001) (Fig. 4B).

On the three remaining copper-coils, one was found in right atrium and the other two coils were not found in the hearts or lungs. The weight of the clot in the right atrium was 3.6 g and the uptake of ^{111}In-64C5 and ^{125}I-DIG26-11 was 0.102 and 0.021 %ID/g, respectively. The total uptake of ^{111}In-64C5 in this clot was 0.37% of the injected dose. This clot was visible in vivo.

Figure 5 is an anterior gamma scintigram of a dog with experimental pulmonary emboli acquired at 24 hr after

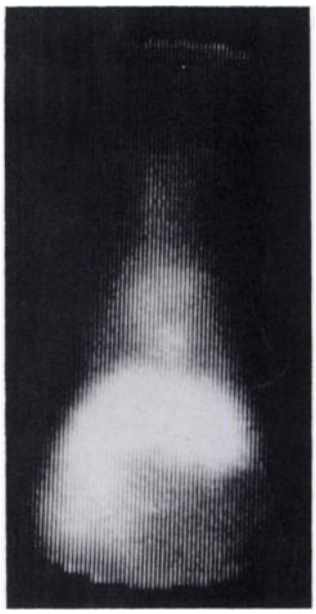

FIGURE 5. A representative 24-hr anterior gamma image of a dog with experimental pulmonary emboli injected intravenous with ^{111}In-labeled control nonantifibrin-specific monoclonal antibody 3H3. Cardiac blood-pool activity is seen clearly, but no hot spots were seen in the region of the lungs.

intravenous administration of ^{111}In-labeled non-fibrin-specific control monoclonal antibody 3H3. Residual blood-pool cardiac activity as well as the hepatic activity can be unequivocally visualized. However, no activity localized in the region of the lungs despite presence of clots confirmed by ex vivo examination. Figure 6 shows a representative example of a set of in vivo gamma images and the corresponding ex vivo image of the lungs. In the anterior view, the clot can be visualized in the right lower lobe of the lungs which is separated from the blood-pool activity, whereas the activity of the same clot appeared to be superimposed on the cardiac blood-pool in the right lateral image. On the other hand, activity in a smaller thrombus can be seen in this view. These two regions of tracer localization in the thrombi are also seen in the ex vivo image of the inflated lungs.

DISCUSSION

Recent studies reported successful in vivo gamma imaging of the blood clots using monoclonal antibodies (*7,8, 19,20*). Unfortunately, these studies were performed using thrombogenic materials, such as copper-coils as the nidus for the clot. Clots formed by these thrombogenic copper-coils may continually entrap circulating proteins, such as antibodies, irrespective of antibody specificity. To determine the role of thrombogenic material on antibody localization, we studied two types of thrombi: (1) barium-thrombin clot and (2) copper-coil clot, in the same animals. A disadvantage of the barium clot model was its tendency to fragment into very small pieces as the primary clots were dislodged from their venous sites. This introduced an unpredictable factor in the total number of clots embolized to pulmonary beds. Despite this drawback, the barium clot model may simulate the clinical situation more accurately than that by the copper-coil model. Fur-

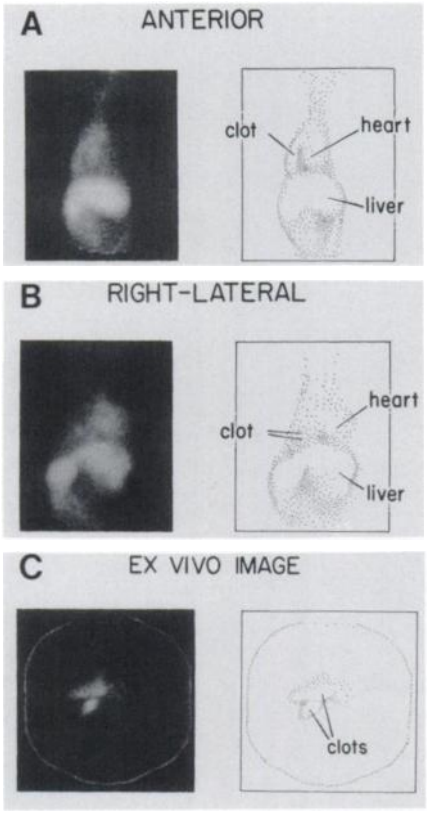

FIGURE 6. Gamma scintigrams of a dog with positive in vivo and ex vivo image detection of pulmonary emboli. (A) anterior image (left panel), (B) right lateral image (left panel), and (C) ex vivo image of the lungs (left panel) and the corresponding diagrammatic representations of the images (right panels).

thermore, the absolute amount of fibrin in the barium clot is reduced, which in turn would reduce the absolute amount of antibody which might be able to bind in a fibrin clot without barium. Since both barium and copper-coils are visible on chest radiographs, the postmortem localization of clot was simplified.

Despite the drawbacks of barium impregnated and copper-coil clots, uptake of ^{111}In-labeled 64C5 was not significantly different in the two types of clot [0.184 ± 0.514 (mean %ID/g ± s.e.m.) and 0.181 ± 0.03, respectively] and the mean uptake of all clots at 24 hr after intravenous administration of the antibody was 0.183 ± 0.105 (mean ± s.e.m.). This mean uptake was greater than uptake of ^{111}In-labeled antifibrin 59D8 Fab (0.074 ± 0.061, mean %ID/g ± s.d.) as reported by Knight and co-workers (*8*). Although both studies utilized the 24-hr postintravenous administration time period for assessment of antibody uptake in the thrombi, the major differences are the use of intact antibody in our study and Fab in the study of Knight and co-workers, which is evidenced by the absolute concentration of antibody localized in the thrombi, and that between pulmonary emboli and venous thrombi. Despite the longer half-life of intact antibodies in the circulation, the mean clot-to-blood activity (mean %ID/g) ratio in our study at 24 hr was 6.78:1, which is very similar to that reported by Knight and co-workers (7.05:1).

We had chosen to use 64C5 rather than 59D8 because of its availability and lower cross-reactivity with alpha-chain peptide of the fibrin monomer (*6*). Both 64C5 and 59D8 were also observed to be cross-reactive with canine fibrin beta-chains (data not shown). Although 64C5 ($5.58 \times 10^6\ M^{-1}$) has a slightly lower relative avidity coefficient than 59D8 (1.45×10^7) (*21*) and since both antibodies were produced in response to immunization by the same peptide antigen, minimal differences were envisioned between the two antibodies.

The blood clearance of ^{111}In-64C5 and ^{125}I-DIG26-11 were not significantly different. The half-life of the slow component of both antibodies was about 14 hr, which is different from the half-life of the slow component of ^{111}In-T2G1s as reported by Rosebrough and co-workers of 33 hr (*19*). The reason for the differences in half-lives is not known. However, the first blood sample to be obtained by these investigators was the 5-min blood sample, and our first sample was obtained at 1 min after intravenous administration of the radiolabeled antibodies. Therefore, the difference in half-lives seen in our study and that of Rosebrough et al. (*19*) may reflect the utilization of the assumption that the first blood sample obtained represented the maximal 100% blood activity, be it at 1 or 5 min, respectively. Since we compared blood clearances of 64C5 to DIG26-11 in the same animals and found them not to be significantly different, we must assume that the half-lives of both these antibodies were correct.

Mean clot uptake of ^{111}In-64C5 (0.183 ± 0.105 mean %ID/g) was significantly higher than that of non-fibrin-specific ^{125}I-DIG26-11 (0.024 ± 0.025) ($p < 0.001$). The results suggest that 64C5 has high specificity for pulmonary clots. There is a direct correlation between clot size and %ID per clot of ^{111}In-64C5 (Fig. 4B). However, uptake represented as %ID/g of clot showed an inverse exponen-

TABLE 1
Individual Clot Uptake of ^{111}In- 64C5 and ^{125}I-DIG26-11

Clot weight (g)	^{111}In-64C5		^{125}I-DIG26-11	
	(%dose/g)	(%dose/clot)	(%dose/g)	(%dose/clot)
0.004–	0.312	0.001	0.088	0.000
0.017–	0.268	0.004	0.009	0.000
0.047*	0.346	0.016	0.013	0.001
0.051+[c]	0.228	0.012	0.015	0.001
0.068+	0.165	0.011	0.045	0.003
0.147–	0.043	0.006	0.012	0.002
0.196+	0.108	0.021	0.015	0.003
0.232–	0.046	0.011	0.008	0.002
0.287+[c]	0.171	0.049	0.016	0.005
0.974+[c]	0.145	0.141	0.023	0.022

[c] = copper-coil clots excluding weight of copper coil.
The rest of the clots were barium impregnated clots.
(in vivo image: + = visible, – = not visible, * = overlapped liver)

tial relationship to clot size (Fig. 4A), indicating that although large clots localized higher absolute amounts of ^{111}In-64C5, on a per gram basis, large clots localized less ^{111}In-64C5. This is probably due to the inaccessibility of ^{111}In-64C5 into the central core of large clots.

The sensitivity of 64C5 by in vivo radioimmunoimaging was only 50% (5 of 10 clots). Although a sixth clot showed a high of 0.346% ID/g activity (Table 1), it was not visualized in vivo due to its position in the lung which overlapped the liver activity. However, it was visualized during the ex vivo imaging of the lungs. The sub-optimal sensitivity may be due to the limits of resolution of the gamma camera which cannot detect very small lesions unless they have either extremely high contrast or high concentration of tracer. The mean weight of visualized clots was 0.315 ± 0.381 g and that of undetected clots was 0.089 ± 0.098 g. Although clot size is important for successful visualization by immunoscintigraphy, the pathology of the clot may also play an important role. The small clots that were not detected by radioimmunoscintigraphy may not have significant pathophysiologic outcome either in man or dog. In a study of 523 consecutive autopsies, 61 cases were found to have pulmonary thromboembolism (*22*). Twenty-five had pulmonary infarction, whereas the rest showed no macro- or microscopic evidence of infarction. The mean diameter of the largest thrombosed vessel in each lobe was 4.9 ± 0.8 mm (mean ± s.e.m.) and 4.6 ± 0.4 mm, respectively. Assuming the density of the clot to be 1.1, and the minimal length of the clots to be 1–2 cm, an average thromboembolus from the group with pulmonary infarction would weigh between ~205 to 411 mg, and ~191 and 381 mg for those without pulmonary infarction. Tsao and co-workers observed thromboemboli to be as long as 5 cm or more and some to be shorter than 3 cm (*23*). These investigators also observed a direct correlation between the diameter of the infarct (cm) and the proximal diameter of the occluded artery (mm). Although there is no direct data to equate the diameter of the involved artery and the length of the thrombus to its weight, it appears that thrombi of 4 and 17 mg may not be pathophysiologically relevant and may well be beyond the sensitivity range for a gamma camera. The reason for not detecting the two larger clots (147 and 232 mg) by in vivo imaging is probably due to low antibody uptake (0.043 and 0.046 %ID/g). The clots which were visualized by in vivo imaging had antibody uptake ranging from 0.108 to 0.228 %ID/g. The smallest visible clot in our study was 51 mg and that of the largest invisible clot was 232 mg, suggesting that size alone is not the factor limiting visualization. Therefore, successful visualization of pulmonary emboli, by gamma imaging may also depend on: (1) whether the clots are occlusive or nonocclusive; (2) the extent of the surface area of the clot accessible for binding by the specific antibodies; and (3) the geographic location of the clot in the lung. Thrombi overlaying a high background region such as the liver may not be visible by planar gamma imaging. Successful visualization of a pulmonary thrombus may also depend on whether the thrombus is undergoing thrombolysis, stable, or thrombogenesis.

Thus, these results suggest that sensitivity of the method for visualization and detection of pulmonary emboli may depend not only on the affinity of the antibody for the clots but also on the pathologic state and environment, such as background due to blood activity in the heart, great vessels, liver, and other organs. Although our study showed a potential for the application of fibrin-specific monoclonal antibodies for the detection of pulmonary emboli, the sensitivity of this technique with our embolic model is insufficient to warrant trials in human subjects with this antibody.

REFERENCES

1. Alderson PO, Doppman JL, Diamond SS, et al. Ventilation-perfusion lung imaging and selective pulmonary angiography in dogs with experimental pulmonary embolism. *J Nucl Med* 1978;19:164–171.
2. Grossman ZD, Wistow BW, McAfee JG et al. Platelets labeled with oxine complexes of Tc-99m and In-111. Localization of experimentally induced vascular lesions. *J Nucl Med* 1978;19:488–491.
3. De Nardo SJ, De Nardo GL. Iodine-123-fibrinogen scintigraphy. *Semin Nucl Med* 1977;7:245–252.
4. Spar IL, Varon MI, Goodland RL, et al. Isotopic detection of thrombi. *Arch Surg* 1966;92:752–758.
5. Spar IL, Perry JM, Benz LL, et al. Detection of left atrial thrombi. Scintillation scanning after administration of I-131 rabbit antibodies to human fibrinogen. *Am Heart J* 1969;78:731–739.
6. Hui KY, Haber E, Matsueda GR. Monoclonal antibodies to a synthetic fibrin-like peptide bind to human fibrin but not fibrinogen. *Science* 1983;222:1129–1132.
7. Kudryk B, Rohoza A, Ahadi M, et al. Specificity of a monoclonal antibody for the NH2-terminal region of fibrin. *Mol Immunol* 1984;21:89–94.
8. Knight LC, Maurer AH, Ammar IA, et al. Evaluation of In-111-labeled antifibrin antibody for imaging vascular thrombi. *J Nucl Med* 1988;29:494–502.
9. Gupta N, Alavi A, Palevshi H, et al. The detection of deep venous thrombi using indium-111-antifibrin monoclonal antibody [Abstract]. *J Nucl Med* 1987;28:1930.
10. Pauwels EKJ, Feitsma RIJ, Nieuwenhuisen W, et al. Imaging of thrombi with Tc-99m-labeled fibrin-specific monoclonal antibody in a rabbit model [Abstract]. *J Nucl Med* 1986;27:975.
11. Rosebrough SF, Kudryk B, Grossman ZD, et al. Radioimmunoimaging of venous thrombi using iodine-131 monoclonal antibody. *Radiology* 1985;156:515–517.
12. Rosebrough SF, Grossman ZD, McAfee JG, et al. Aged venous thrombi: radioimmunoimaging with fibrin-specific monoclonal antibody. *Radiology* 1987;162:575–577.
13. Matsueda GR, Haber E. The use of an internal reference amino acid for the evaluation of reactions in solid-phase peptide synthesis. *Anal Biochem* 1980;104:215–227.
14. Matsueda GR, Haber E, Margolies MN. Quantitative solid-phase amino degeneration for evaluation of extended solid-phase peptide synthesis. *Biochem* 1981;20:2571–2580.
15. Ey PL, Prowse SJ, Jenkin CR. Isolation of pure IgG1, IgG2a, IgG2b immunoglobulins from mouse serum using protein A-Sepharose. *Immunochem* 1978;14:429–436.
16. Laemmli UK. Cleavage of structural proteins during the assembly of the head of bacteriophage T4. *Nature* 1970;227:680–685.
17. Krejcarek GE, Tucker KL. Covalent attachment of chelating groups to macromolecules. *Biochem Biophys Res Comm* 1977;77:581–585.
18. Marchalonis JJ. An enzymatic method for the trace iodination of immunoglobulins and other proteins. *Biochem J* 1969;113:299–305.
19. Rosebrough SF, Kudryk B, Grossman ZD, et al. Radioimmunoimaging of venous thrombi using indium-111-monoclonal antibody. *Radiology* 1985;156:515–517.

20. Oster ZH, Srivastava SC, Som P, et al. Thrombus radioimmunoscintigraphy: an approach using monoclonal antiplatelet antibody. *Proc Natl Acad Sci* 1985;82:3465–3468.
21. Liau CS, Haber E, Matsueda GR. Evaluation of monoclonal antifibrin antibodies by their binding to human blood clots. *Thromb Haemost* 1987;57:49–54.
22. Schraufnagel DE, Tsao MS, Yao YT, Wang NA. Factors associated with pulmonary infarction. *Am J Clin Pathol* 1985;84:15–18.
23. Tsao MS, Schraufnagel DE, Wang NA. Pathogenesis of pulmonary infarction. *Am J Med* 1982;72:599–606.

(continued from p. 1238)

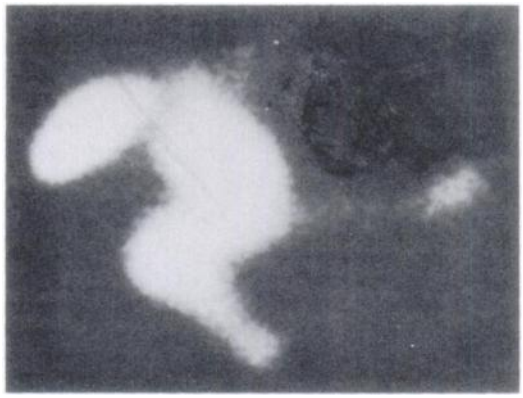

Post-CCK
Figure 4

4. You are shown images obtained with ^{99m}Tc-disofenin before and after administration of cholecystokinin (Fig. 5A) and a gallbladder emptying curve (Fig. 5B) from a patient with recurrent right upper quadrant pain and a normal sonogram of the gallbladder and bile ducts. The first image in this sequence was taken 60 minutes after injection of ^{99m}Tc-disofenin. Which *one* of the following is the best interpretation of this study?

A. acute cholecystitis
B. chronic acalculuous cholecystitis
C. sphincter of Oddi dyskinesia
D. bile gastritis
E. normal study

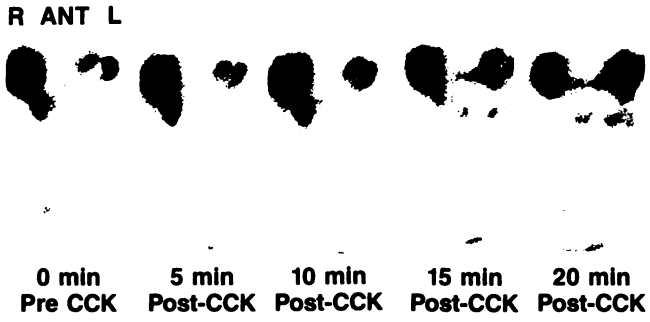

Figure 5A

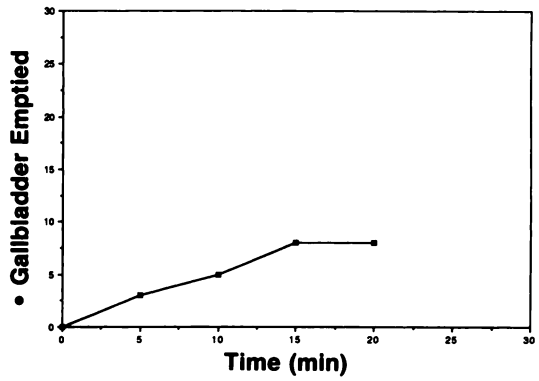

Figure 5B

SELF-STUDY TEST
Gastrointestinal Nuclear Medicine
ANSWERS

ITEMS 1 and 2: Bile Leak

ANSWERS: 1, D; 2, E

Following blunt injury to the abdomen, there may be hepatic laceration or fracture, with resultant disruption of the biliary tree. Cholescintigraphy is a useful method of determining the presence of a biliary leak or formation of a bile cyst (biloma).

The images in Figure 1 show rapid uptake of the tracer by the liver. On the immediate postinjection image, the left lobe of the liver has patchy uptake and irregular margins. With time, a small "nubbin" of activity is seen in the central portion of the left lobe. These findings likely represent disruption (laceration) of the left lobe of the liver, with resultant severance of the left hepatic duct. Over time, the common bile duct is visualized, with free transit of the radiotracer into the duodenum. By 45 minutes, the gallbladder is faintly visualized, and continues to accumulate the radiotracer thereafter. Therefore neither acute nor chronic cholecystitis is likely.

Immediately adjacent to the left lobe of the liver, a collection of activity is apparent at 30 minutes; this collection becomes more prominent over time, has a roughly triangular configuration, and persists on the 24-hour image (Fig. 2). This likely represents leakage of bile into the confines of the lesser sac. Since the majority of bile is draining into the small bowel, however, the patient can be managed conservatively and no specific therapy is necessary. Neither an intravenous cholangiogram or CT scan is needed, as the scintigraphic pattern is diagnostic of a bile leak.

While penetrating injury is usually managed by surgical intervention, blunt biliary trauma is managed conservatively, since initially hemorrhage is the main concern. In most individuals, disrupted bile ducts probably heal spontaneously, but some individuals will go on to form an enclosed bile cyst (or biloma). Formation of a bile cyst may be preceded by a latent period occurring after the initial injury, after which the individual gradually develops symptoms. Bile cysts usually involve the right lobe of the liver, may be quite large, and may or may not communicate with the biliary tree.

Following surgery, cholescintigraphy is particularly useful in determining that a patient's recurrent symptoms are due to bile leakage. A frequent cause of leakage is incomplete cystic duct ligation, and hence, the most common location of the bile collection is the gallbladder fossa, although a collection may form in any dependent portion of the peritoneal cavity. In such cases, delayed views are usually necessary to identify the bile

(continued on p. 1317)